

# Computing distances on Riemann surfaces

Huck Stepanyants,<sup>1,2</sup> Alan Beardon,<sup>3</sup> Jeremy Paton,<sup>1,2</sup> and Dmitri Krioukov<sup>1,2,4,5</sup>

<sup>1</sup>*Department of Physics, Northeastern University, Boston, Massachusetts 02115, USA*

<sup>2</sup>*Network Science Institute, Northeastern University, Boston, Massachusetts 02115, USA*

<sup>3</sup>*Department of Pure Mathematics and Mathematical Statistics,  
University of Cambridge, Cambridge CB3 0WB, UK*

<sup>4</sup>*Department of Mathematics, Northeastern University, Boston, Massachusetts 02115, USA*

<sup>5</sup>*Department of Electrical and Computer Engineering,  
Northeastern University, Boston, Massachusetts 02115, USA*

Riemann surfaces are among the simplest and most basic geometric objects. They appear as key players in many branches of physics, mathematics, and other sciences. Despite their widespread significance, how to compute distances between pairs of points on compact Riemann surfaces is surprisingly unknown, unless the surface is a sphere or a torus. This is because on higher-genus surfaces, the distance formula involves an infimum over infinitely many terms, so it cannot be evaluated in practice. Here we derive a computable distance formula for a broad class of Riemann surfaces. The formula reduces the infimum to a minimum over an explicit set consisting of finitely many terms. We also develop a distance computation algorithm, which cannot be expressed as a formula, but which is more computationally efficient on surfaces with high genres. We illustrate both the formula and the algorithm in application to generalized Bolza surfaces, which are a particular class of highly symmetric compact Riemann surfaces of any genus greater than 1.

## I. INTRODUCTION

Riemann surfaces [1] are one of the simplest geometric objects, with widespread applications in physics, mathematics, network science, and other areas. In physics, Riemann surfaces appear naturally in dynamical systems. The simplest example is billiards [2, 3], i.e., a freely moving ball confined to a polygon-shaped table, and bouncing off its sides. This system is equivalently formulated as a particle moving along a straight line on a compact Riemann surface. In particular, a particle moving on the Bolza surface, a compact Riemann surface of genus  $g = 2$ , is one of the simplest and earliest chaotic systems studied in physics [4].

Riemann surfaces also appear in integrable systems [5, 6]. The trajectory of such a system in its parameter space is effectively confined to a Riemann surface. Elsewhere in mathematical physics, Riemann surfaces are a part of string theory [7, 8], potential theory [9, 10], and approximation theory [11–13]. In quantum physics, Riemann surfaces appear in the study of fractional quantum Hall states [14], spin liquids [15], and quantum gravity [16, 17].

In network science, Riemann surfaces have been used as latent spaces in some models of networks. For example, networks embedded in hyperbolic spaces are one of the first models that reproduce a collection of the most basic properties common to many real-world networks [18]. Yet our main motivation for this paper comes from [19, 20], where the convergence of the Ollivier curvature [21] of random geometric graphs [22, 23] to the Ricci curvature of their underlying Riemannian manifolds was

proven. Vertices in such graphs are random points in a Riemannian manifold, and pairs of vertices are connected by edges if the distance between the two vertices in the manifold is below a fixed threshold. To build a random geometric graph in a manifold, one thus needs to be able to compute distances between pairs of points in it.

Compact Riemann surfaces are two-dimensional Riemannian manifolds. They can be equipped with a metric which defines the distance between a pair of points on the surface. Genus  $g = 0$  (sphere),  $g = 1$  (torus), and  $g \geq 2$  surfaces admit the spherical, euclidean, and hyperbolic metrics, respectively. While computing distances on the first two of these surfaces is trivial, the task is much more difficult on a hyperbolic Riemann surface, where the distance is given as an infimum over a countably infinite number of geodesics, i.e., locally minimal paths. There are no formulas for the distance between points on any genus  $g \geq 2$  surface which are computable in finite time. To be precise, while it is known that the mentioned infimum is actually a minimum since only a finite set of geodesics needs to be considered (Prop. 2.1, [24]), it is not known what this set actually is for any  $g \geq 2$  surface, which is surprising since distance plays a crucial role in many applications of these surfaces mentioned above.

Here we compute distances on Riemann surfaces obtained by pairing the sides of a convex hyperbolic polygon. We obtain an expression for a finite set of geodesics whose minimum gives the correct distance between any two points on these surfaces. This leads to a distance formula which can be evaluated in finite time. We also develop a fast algorithm for

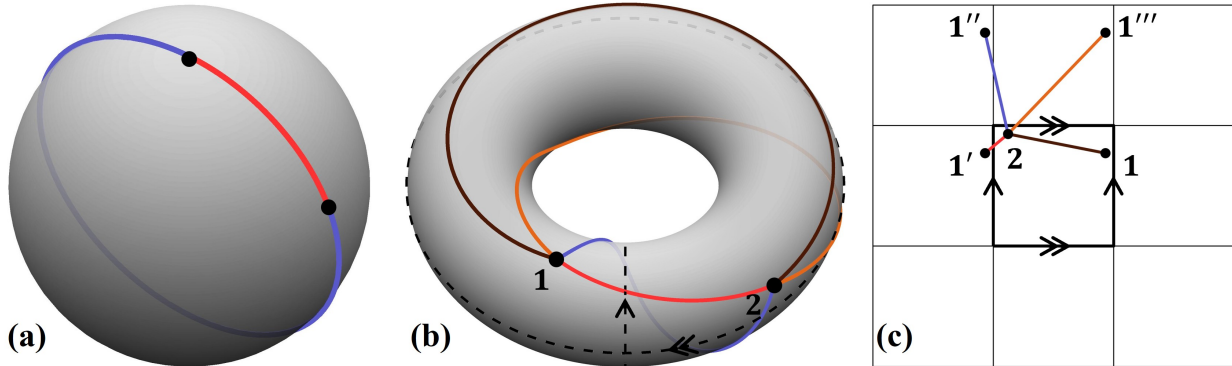


FIG. 1. (a) The two geodesic paths connecting a given pair of points on a sphere. (b) A topological representation of the 2D torus  $\mathbb{R}^2/\mathbb{Z}^2$ . The dashed lines are its “seams.” Cutting the torus along these seams produces the square in (c). The colored solid lines indicate four of the infinitely many geodesic paths connecting the pair of points 1, 2. (c) The corresponding points and geodesics in the  $\mathbb{R}^2$  representation of the torus. The highlighted central square is a fundamental domain of the torus and the arrows indicate its side pairing. The distance between point 1 and 2 on the torus is between 2 and the image 1' of point 1 on  $\mathbb{R}^2$ .

computing distances on these surfaces using a different set of ideas. For illustrative purposes, we show how the formula and the algorithm can be applied to computing distances on generalized Bolza surfaces [25]. These are highly symmetric hyperbolic Riemann surfaces of any genus  $g \geq 2$ . We prove that the time required to evaluate the formula in this case is  $O(g^{\alpha \log g})$ , where  $\alpha \approx 1.52$ , and show experimentally that the time required to run the algorithm is  $O(g^4)$ .

In Sec. II, we provide necessary background information on Riemann surfaces, and a detailed introduction to the distance problem. In Sec. III and IV, we present and discuss our results, a formula and an algorithm, respectively, for computing distances on Riemann surfaces. In Sec. V, we apply our results to generalized Bolza surfaces, and evaluate the resulting running times.

## II. BACKGROUND AND DEFINITIONS

The distance between two points in a space is the length of the shortest geodesic, or locally minimal path, that connects them in the space. If the space is a compact Riemann surface, then the number of geodesics connecting a given pair of points depends on its *genus*, which is the number of holes the surface has. Given two points on the genus 0 sphere (Fig. 1(a)), there are always two geodesics between them, and thus the distance is simply a minimum of two lengths. In contrast, the number of geodesics between two points on the torus  $\mathbb{R}^2/\mathbb{Z}^2$  is infinite (four are shown in Fig. 1(b)), which could make computing distances on the torus difficult. Nevertheless,

due to its symmetry, the distance  $d$  on the torus is given by the simple formula:

$$d^2 = \left( \frac{1}{2} - \left| \frac{1}{2} - |x_1 - x_2| \right| \right)^2 + \left( \frac{1}{2} - \left| \frac{1}{2} - |y_1 - y_2| \right| \right)^2, \quad (1)$$

where  $(x_1, y_1)$  and  $(x_2, y_2) \in [-1/2, +1/2]^2$  are the coordinates of the representatives of two points on the torus, which is the unit square with vertices at  $(\pm 1/2, \pm 1/2)$  whose opposite sides are paired, Fig. 1(c). For genus  $g > 1$  (hyperbolic) surfaces, the number of geodesic paths connecting two points is also infinite. Yet there are no closed-form distance formulas analogous to Eq. (1) for any of these surfaces.

Here, we address the distance problem for the hyperbolic Riemann surfaces known as *quotient surfaces*. A quotient surface is constructed by taking the quotient of the hyperbolic plane  $\mathbb{H}^2$  with respect to a discrete subgroup of its isometries, or distance-preserving transformations, called a *Fuchsian group*, which we describe next.

We will use the Poincaré disk model of  $\mathbb{H}^2$ , which is the complex unit disk equipped with the metric

$$ds^2 = \frac{4dzd\bar{z}}{(1 - |z|^2)^2}. \quad (2)$$

The group of orientation-preserving isometries of the Poincaré disk is the projective special unitary group  $\text{PSU}(1, 1)$ , the quotient of the special unitary group  $\text{SU}(1, 1)$  by its center  $\{I, -I\}$ . In matrix form,

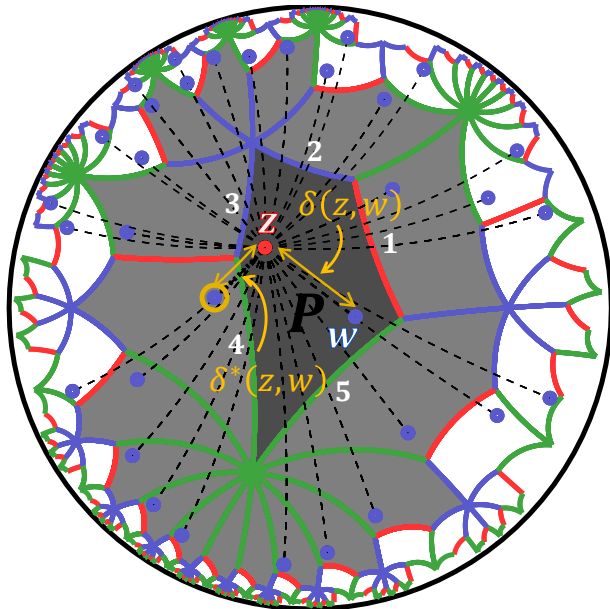


FIG. 2. Quotient surface obtained by pairing the sides of a nonregular pentagon in the order  $1 \leftrightarrow 1$ ,  $2 \leftrightarrow 3$ ,  $4 \leftrightarrow 5$ . The generators of the Fuchsian group  $\Gamma$  map the fundamental polygon  $P$  (dark gray) to its edge-adjacent neighbors (light gray). To compute the distance  $\delta^*(z, w)$  between a pair of points  $z$  and  $w$  on the surface, the lengths  $\delta(z, \gamma w)$  of the infinite number of geodesics between  $z$  (red dot) and all of the images  $\gamma w$  (blue dots) of  $w$ ,  $\forall \gamma \in \Gamma$ , on the hyperbolic plane  $\mathbb{H}^2$  must be considered. The shortest such distance, between  $z$  and the circled image of  $w$  in the figure, is then  $\delta^*(z, w)$ .

these isometries are

$$\gamma = \begin{bmatrix} a & \bar{c} \\ c & \bar{a} \end{bmatrix}, \quad \forall a, c \in \mathbb{C} : |a|^2 - |c|^2 = 1, \quad (3)$$

which act on points  $z \in \mathbb{C}$  via fractional linear transformations,

$$\begin{bmatrix} a & \bar{c} \\ c & \bar{a} \end{bmatrix} (z) = \frac{az + \bar{c}}{cz + \bar{a}}. \quad (4)$$

A subgroup  $\Gamma$  of the isometry group  $\text{PSU}(1,1)$  is called *Fuchsian* if it acts discontinuously on  $\mathbb{H}^2$ . This means that for any point  $z$ , the orbit  $\Gamma z$  has no *accumulation points*  $w$ ,  $|w| < 1$ . An accumulation point  $w$  is one for which there are elements of  $\Gamma z$  in any arbitrarily small punctured disk around  $w$ . Every Fuchsian group defines a quotient surface,

$$S = \mathbb{H}^2 / \Gamma. \quad (5)$$

Points  $[z]$  on  $S$  are orbits of points  $z$  in  $\mathbb{H}^2$  under

actions by  $\Gamma$ ,

$$[z] = \Gamma z. \quad (6)$$

The distance  $\delta^*(z, w)$  between two points  $[z]$  and  $[w]$  on  $S$  is a distance between orbits  $\Gamma z$  and  $\Gamma w$  in  $\mathbb{H}^2$ . It is given by

$$\begin{aligned} \delta^*(z, w) &= \inf_{\gamma_1, \gamma_2 \in \Gamma} \delta(\gamma_1 z, \gamma_2 w) \\ &= \inf_{\gamma \in \Gamma} \delta(z, \gamma w), \end{aligned} \quad (7)$$

where  $\delta$  is the distance in  $\mathbb{H}^2$ . This formula cannot be directly evaluated, since  $\Gamma$  has infinitely many elements. To find  $\delta^*(z, w)$ , one must consider infinitely many geodesics from  $z$  to  $\gamma w$ . Every such geodesic corresponds to a different minimal path between the same pair of points on  $S$ , like those illustrated in Fig. 1 for the sphere and torus, or in Fig. 6 for the Bolza surface.

Here we will focus on surfaces  $S$  whose Fuchsian groups  $\Gamma$  are finitely generated and of the *first kind*. The latter means that any point on the boundary of the unit disk, which is the boundary at infinity of the hyperbolic plane  $\mathbb{H}^2$ , is an accumulation point of some orbit of  $\Gamma$ . This guarantees that  $S$  is a compact surface, and by Theorem 10.1.2 in [26],  $S$  has a convex *fundamental* polygon  $P$  with a finite number of sides. A fundamental polygon is one that contains exactly one representative of each point on  $S$ , see Fig. 2. It is known [26] that in such settings, the generators of the group  $\Gamma$  pair sides of  $P$  by mapping it to its edge-adjacent neighbors, shown in light gray in Fig. 2. We will further assume that  $P$  does not have any vertices at infinity.

Using the geometry of  $P$ , we develop two methods for computing distances on  $S$ . In the next Sec. III, we present a distance formula which reduces the infinities in Eq. (7) to finite sets. Then in Sec. IV, we develop a more efficient algorithmic approach to the problem.

### III. DISTANCE FORMULA

Let  $S$  be a quotient surface obtained by pairing the sides of a convex fundamental polygon  $P$ , and let  $\Gamma$  denote its Fuchsian group. Let  $z$  and  $w$  be representatives of two points on the surface. In this section we obtain a computable version of Eq. (7), where instead of minimizing  $\delta(z, \gamma w)$  over all  $\gamma \in \Gamma$ , we minimize over a finite subset  $\Gamma_0 \subset \Gamma$ . We will derive a formula for  $\Gamma_0$  using the geometry of  $P$ .

Let us call a pair of images of  $P$  *neighbors* if they share either a common edge or a common vertex. Let  $T \subset \Gamma$  denote the subset of isometries from the Fuchsian group which map  $P$  to all of its neighbors

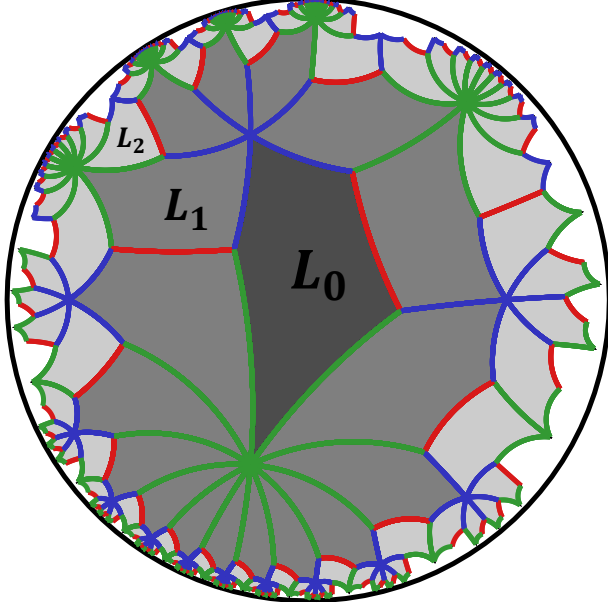


FIG. 3. Shells  $L_0 = P$  (dark gray),  $L_1$  (medium gray), and  $L_2$  (light gray).

and itself. Then we define the  $k^{\text{th}}$  shell  $L_k$ , for  $k \geq 1$ , to be the difference

$$\bigcup_{\gamma \in T^k} \gamma P \setminus \bigcup_{\gamma \in T^{k-1}} \gamma P, \quad (8)$$

and for  $k = 0$ , we define  $L_0 = P$ , as illustrated in Fig. 3.

We next compute an upper bound on the minimum value of  $k$ ,  $k_{\min}$ , for which the correct value of the distance  $\delta^*(z, w)$  is obtained by minimizing  $\delta(z, \gamma w)$  over  $\forall \gamma \in T^k$ . Thus  $k_{\min}$  is the minimum positive integer  $k$  satisfying

$$\delta^*(z, w) = \min_{\gamma \in T^k} \delta(z, \gamma w) \quad (9)$$

for all  $z$  and  $w$ . In other words, the finite subset  $\Gamma_0 \subset \Gamma$  mentioned above can be taken to be

$$\Gamma_0 = T^{k_{\min}}. \quad (10)$$

We bound  $k_{\min}$  for an arbitrary surface by the ratio of two distances: the surface diameter  $\mathcal{D}$ , i.e., the maximum possible distance between two points on the surface, and the minimal distance  $\mathcal{T}$  required to traverse a shell. *To traverse* here means *to cross* from the outer boundary of  $L_k$  to the outer boundary of  $L_{k+1}$  for  $k \geq 0$ . In Appendix A, we show that this distance does not depend on  $k$ , and satisfies the inequality

$$\mathcal{T} \geq \min(\delta, 2\epsilon), \quad (11)$$

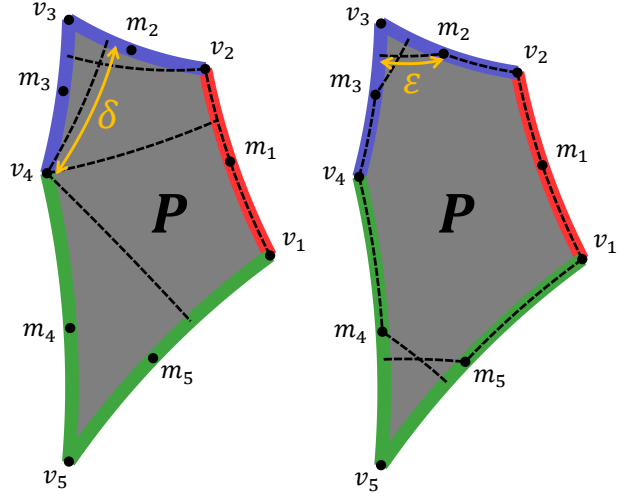


FIG. 4. **Left:** Shortest paths between nonadjacent sides whose minimum gives  $\delta$ . **Right:** Shortest paths from the midpoint of a side to an adjacent edge whose minimum gives  $\epsilon$ .

where  $\delta$  is the minimum distance between any pair of non-adjacent sides of  $P$ , and  $\epsilon$  is the minimum distance from the midpoint of an side to any adjacent side as illustrated in Fig. 4.

Then the distance required to cross from a starting point in  $L_0 = P$  to a point in  $L_k$  is lower-bounded by  $(k-1)\mathcal{T}$ . Since  $\mathcal{D}$  is the surface diameter, then  $k_{\min}$  must satisfy the inequality

$$(k_{\min} - 1)\mathcal{T} < \mathcal{D}. \quad (12)$$

But the surface diameter  $\mathcal{D}$  is trivially upper bounded by the diameter of its fundamental polygon  $P$ ,  $\text{diam}(P)$ :

$$\mathcal{D} \leq \text{diam}(P) = \max_{ij} \delta(v_i, v_j), \quad (13)$$

where the  $v_i$  are the vertices of  $P$ . Combining Eqs. (11), (12), and (13) leads to an upper bound on  $k_{\min}$  in terms of geometric properties of  $P$ , which we denote  $k^*$ :

$$k_{\min} \leq k^* = \left\lceil 1 + \frac{\max_{ij} \delta(v_i, v_j)}{\min(\delta, 2\epsilon)} \right\rceil. \quad (14)$$

Substituting this bound in Eq. (9) yields an explicit computable formula for the distance between a pair of points on the surface:

$$\delta^*(z, w) = \min_{\gamma \in T^{k^*}} \delta(z, \gamma w). \quad (15)$$

#### IV. DISTANCE ALGORITHM

In this section, we present an algorithm to compute  $\delta^*(z, w)$  by minimizing  $\delta(z, \gamma w)$  over an even smaller subset of  $\Gamma$ . This subset depends on the location of  $z$  and is unknown *a priori*—instead, it is constructed via a search over the polygon tessellation. As we will see in Sec. V, this method is generally more computationally efficient than evaluating the distance formula in Sec. III.

Let  $N$  be the number of sides of  $P$ , and  $g_i$ ,  $i = 1, 2, \dots, N$ , be the generators of  $\Gamma$  and their inverses. With these notations, the algorithm is:

---

**Algorithm 1** Distance calculation.

---

```

 $\Delta \leftarrow \{1\}, \gamma_{\min} \leftarrow 1$ 
while  $|\Delta| > 0$  do
   $\gamma \leftarrow \text{pop}(\Delta)$ 
  if  $\delta(z, \gamma w) < \delta(z, \gamma_{\min} w)$  then
     $\gamma_{\min} \leftarrow \gamma$ 
  end if
  for  $i = 1 : N$  do
    if  $\delta(z, \gamma P) < \delta(z, \gamma g_i P) < \text{diam}(P)$  then
       $\Delta \leftarrow \text{push}(\gamma g_i)$ 
    end if
  end for
end while
return  $\gamma_{\min}$ 

```

---

This algorithm is a depth-first search for an image  $\gamma w$  of  $w$ ,  $\gamma \in \Gamma$ , that minimizes  $\delta(z, \gamma w)$ , in the polygon tessellation  $\Gamma P$  illustrated in Fig. 5. We keep track of two variables: the list of isometries  $\Delta \subset \Gamma$  corresponding to the polygons to be searched next, and the current best solution  $\gamma_{\min}$  that minimizes  $\delta(z, \gamma w)$  across all  $\gamma$  searched so far. Both  $\Delta$  and  $\gamma_{\min}$  are initialized to the identity:  $\Delta = \{1\}$ ,  $\gamma_{\min} = 1$ , corresponding to  $P$  itself.

At every step of the search, we set  $\gamma$  to be the last element of  $\Delta$ , and remove it from  $\Delta$ . If  $\delta(z, \gamma w) < \delta(z, \gamma_{\min} w)$ , we update  $\gamma_{\min}$  to  $\gamma$ . We then append to  $\Delta$  the group elements  $\gamma g_i$ ,  $1 \leq i \leq N$ , corresponding to polygons that are edge-adjacent to the currently searched polygon, but only if they are at a greater distance from  $z$ :

$$\delta(z, \gamma P) < \delta(z, \gamma g_i P) < \text{diam}(P). \quad (16)$$

Here, the distances  $\delta(z, \gamma P)$  and  $\delta(z, \gamma g_i P)$  from  $z$  to the polygons  $\gamma P$  and  $\gamma g_i P$  are defined to be the minimum distance from  $z$  to one of their sides, with the exception  $\delta(z, P) = 0$ .

The reason to consider only those polygons that increase the distance from  $z$  is as follows. Consider a geodesic from  $z$  to  $\gamma w$ , where  $\gamma \neq 1$ . It intersects

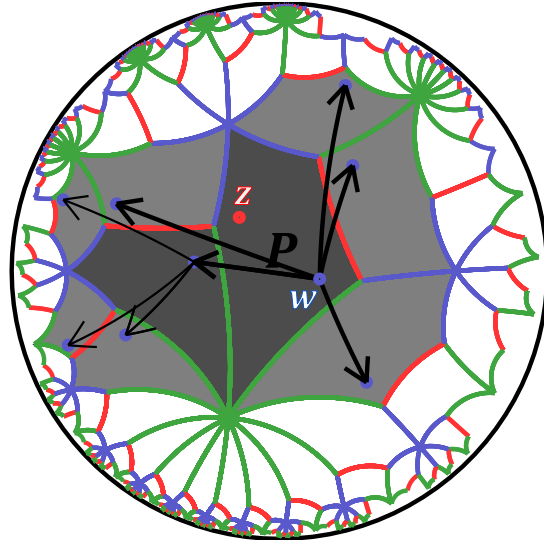


FIG. 5. Illustration of one branch of the depth-first search algorithm. The search starts at the fundamental polygon  $P$  and progresses outward. At every step, the distance from  $z$  to all edge-adjacent polygons (light gray) of the last searched polygon (dark gray) are computed, and those polygons are added to the list  $\Delta$  if and only if they are at a greater distance from  $z$ . The branch terminates when this distance exceeds the diameter of  $P$ .

an edge-adjacent polygon of  $\gamma P$ . This edge-adjacent polygon is closer to  $z$  than  $\gamma P$ . Continuing in this way, we construct a chain of edge-adjacent polygons leading from  $\gamma P$  to  $P$  along which the distance to  $z$  is decreasing, which guarantees that  $\gamma_{\min} P$  will be reached in the search.

The reason not to search the polygons  $\gamma P$  for which  $\delta(z, \gamma P)$  exceeds  $\text{diam}(P)$  is this:

$$\begin{aligned} \delta(z, \gamma_{\min} P) &\leq \delta(z, \gamma_{\min} w) \\ &\leq \mathcal{D} \\ &\leq \text{diam}(P), \end{aligned} \quad (17)$$

where  $\gamma_{\min}$  is the group element we are looking for, i.e., the one that minimizes  $\delta(z, \gamma w)$ , and  $\mathcal{D}$  is the surface diameter.

Finally, the condition in Eq. (16) ensures that the search terminates after a finite time. To see this, let  $M$  denote the number of polygons within the distance  $\text{diam}(P)$  from  $z$ . Note that the number of branches of the search cannot exceed the number of sequences of such polygons ordered by increasing distance, which is  $2^M$ . Therefore, the number of polygons searched does not exceed  $M \cdot 2^M$ . We also consider a total of  $N$  nearest neighbors of  $\gamma P$  at every search step, even though not all of these neighbors

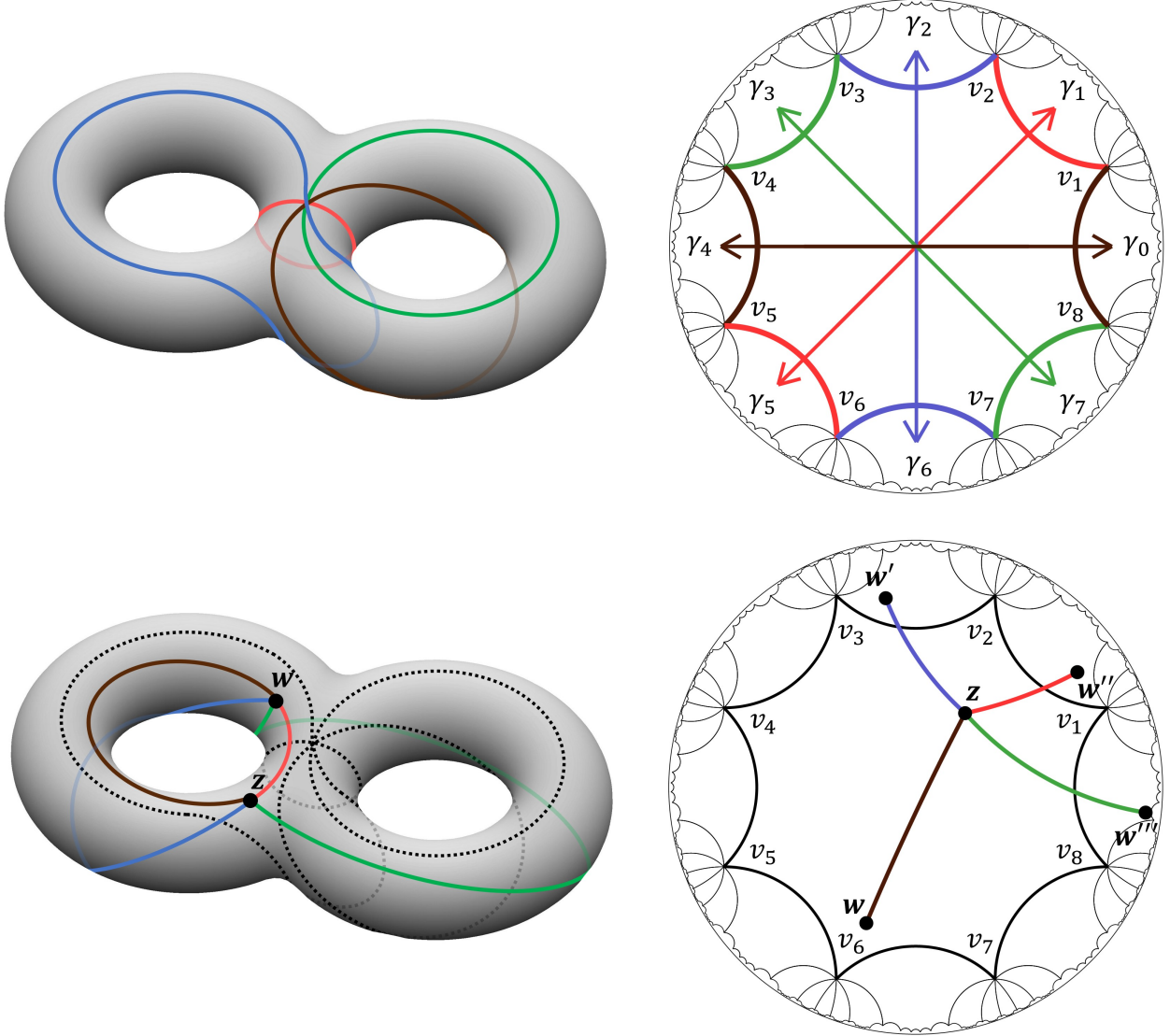


FIG. 6. **Top Left:** A topological representation of the Bolza surface  $S_2$ . The colored lines indicate its “seams,” cutting which and unfolding the surface produces the octagon on the right. **Top Right:** The  $\mathbb{H}^2$  representation of  $S_2$ . The colors indicate its side pairing, and arrows show the action of the generators  $\gamma_i$ ,  $i = 0, 2, \dots, 7$  on the fundamental domain. **Bottom Left:** Four of the infinitely many geodesic paths connecting two points on  $S_2$ . The dashed lines are the seams at the top. **Bottom Right:** The corresponding points and geodesics in the  $\mathbb{H}^2$  representation of  $S_2$ . The distance between points  $z$  and  $w$  on the surface is between  $z$  and the image  $w''$  of  $w$  on  $\mathbb{H}^2$ .

are added to  $\Delta$ . Therefore the total number of steps in the algorithm is  $O(NM \cdot 2^M)$ . In practice, however, we find that the number of steps is  $O(NM)$ , implying that most polygons are searched only  $O(1)$  times, as discussed in the next section.

## V. APPLICATION TO GENERALIZED BOLZA SURFACES

In this section, we apply our general results to the *generalized Bolza surfaces* [25], highly symmetric surfaces of any genus  $g \geq 2$ . We denote them by  $S_g$ .  $S_2$  is known as the Bolza surface [27].

The generalized Bolza surface  $S_g$  has as its fundamental polygon  $P$  the regular  $4g$ -gon with interior

angles  $\pi/2g$  and vertices

$$v_k = \tanh(R/2) \exp\left(\left(k - \frac{1}{2}\right) \frac{\pi i}{2g}\right), \quad (18)$$

$$k = 0, 1, \dots, 4g - 1,$$

where  $R$  is the radius of  $P$ , which satisfies

$$\cosh R = \cot^2\left(\frac{\pi}{4g}\right). \quad (19)$$

The Fuchsian group  $\Gamma_g$  of  $S_g$  is generated by the following  $2g$  isometries (Fig. 6), which pair opposite sides of the fundamental polygon:

$$\gamma_k = \begin{bmatrix} 1 & \tanh\left(\frac{s}{2}\right) e^{\frac{k\pi i}{2g}} \\ \tanh\left(\frac{s}{2}\right) e^{-\frac{k\pi i}{2g}} & 1 \end{bmatrix}, \quad (20)$$

$$k = 0, 1, \dots, 2g - 1,$$

where  $s$  is the length of a side of  $P$ , which satisfies

$$\cosh\left(\frac{s}{2}\right) = \cot\left(\frac{\pi}{4g}\right). \quad (21)$$

Applying the distance formula to these surfaces, we observe that  $\delta < 2\epsilon$  (cf. Fig. 4), and then upper bound  $\delta$  using hyperbolic trigonometry to obtain

$$\min\{\delta, 2\epsilon\} = \delta < \operatorname{arccosh}\left(2 \cos\left(\frac{\pi}{2g}\right)\right). \quad (22)$$

The diameter  $\mathcal{D}_g$  of  $S_g$  is known [28],

$$\mathcal{D}_g = \operatorname{arccosh}\left(\cot\left(\frac{\pi}{4g}\right)\right), \quad (23)$$

and therefore we can substitute the actual diameter, instead the upper bound in Eq. (13), into Eq. (14) for  $k^*$  to obtain

$$k^* = \left\lceil 1 + \frac{\operatorname{arccosh}\left(\cot\left(\frac{\pi}{4g}\right)\right)}{\operatorname{arccosh}\left(2 \cos\left(\frac{\pi}{2g}\right)\right)} \right\rceil. \quad (24)$$

The number of polygons in  $T^{k^*}$  is upper bounded by the number of sequences of  $2k^*$  generators,

$$|T^{k^*}| < (4g)^{2k^*}, \quad (25)$$

and since  $k^* \approx \log g / \operatorname{arccosh} 2$  for large  $g$ , the time required to evaluate the distance formula is  $O(g^{\alpha \log g})$ , where  $\alpha = 2 / \operatorname{arccosh} 2 \approx 1.52$ .

For the Bolza surface  $S_2$ , evaluating Eq. (24) yields  $k^* = 2$ , but in Appendix B we compute  $k_{\min}$  exactly using different methods:

$$k_{\min} = 1. \quad (26)$$

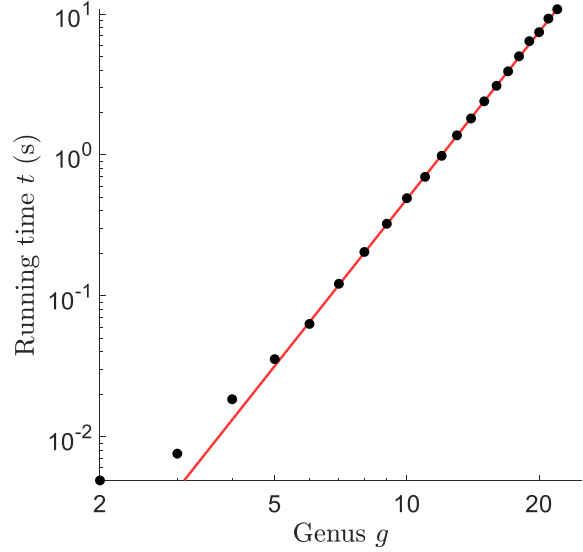


FIG. 7. Distance algorithm running time  $t$  on generalized Bolza surfaces  $S_g$  for  $g = 2, \dots, 100$ . The red line shows the linear fit of the running times and has slope 3.94.

Therefore, the number of  $P$ 's images one must search through to compute the distance is  $|T^{k_{\min}}| = 49$ , corresponding to all polygons adjacent to  $P$  via either a side or a vertex.

To apply the distance algorithm, we substitute the diameter of the surface for  $\operatorname{diam}(P)$  in Algorithm 1, and find experimentally in Fig. 7 that the algorithm running time is  $O(g^4)$ . We cannot prove this observation because we cannot estimate the overcount—the average number of times the same polygon is searched. However, we can show that a maximum of  $O(g^4)$  polygons can intersect a hyperbolic circle of radius  $R$ . Therefore, Fig. 7 indicates that each polygon is searched  $O(1)$  times, so overcounting appears to be minimal.

## Appendix A: Lower bound on $\mathcal{T}$

In this section, we prove an upper bound on the shell-crossing distance  $\mathcal{T}$  for any quotient surface  $S$  obtained by pairing the sides of a convex polygon  $P$ .

This distance is

$$\mathcal{T} = \min \left\{ \delta(\partial T^n(P), \partial T^{n+1}(P)), \quad n \geq 0 \right\},$$

where  $L_n = T^n(P)$  is the  $n^{\text{th}}$  shell,  $T \subseteq \Gamma$  is the set consisting of all maps from  $P$  to an edge- or vertex-

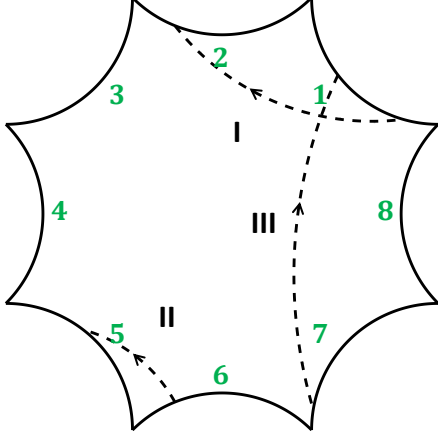


FIG. 8. Type I, II, and III segments (dotted black lines), and edge labels (green).

adjacent polygon and the identity, and  $\partial L_n$  is the boundary of  $L_n$ .

First, observe that for  $\gamma \in T^n$  we have

$$\gamma(P) \subseteq \gamma T(P) \subseteq L_{n+1}.$$

Hence,

$$\delta(\partial\gamma(P), \partial(\gamma T(P))) \leq \delta(\partial\gamma(P), \partial L_{n+1}).$$

Since  $\mathcal{T}$  is the minimum of the right hand side over all  $n \geq 0$  and  $\gamma \in T^n$ , and the left hand side is equal to  $\delta(\partial P, \partial(T(P)))$ , which is  $\geq \mathcal{T}$  by definition of  $\mathcal{T}$ , we conclude that

$$\mathcal{T} = \delta(\partial P, \partial(T(P))).$$

Next, we introduce edge labels, which are positive integers modulo the number  $N$  of distinct (in the quotient sense) sides of  $L_0$ . First, the label 1 is assigned to an edge of  $L_0$  without loss of generality. Then, the  $N - 1$  edges to the left of this edge are labeled  $2, 3, \dots, N - 1$  (Fig. 8). Finally, these labels are copied onto all images of  $L_0$  via the elements of the Fuchsian group  $\mathcal{F}$ . Thus, edges are distinct in the quotient sense if and only if they have different labels. The process of filling in labels, which we call *label chasing*, will be useful later.

Now we will prove the main result of this section:

$$\mathcal{T} \geq \min \left( \{ \delta_{ij}, |i - j| \neq 0, 1 \} \cup \{ 2\epsilon_k \} \right), \quad (\text{A1})$$

where  $\delta_{ij}$  denotes the distance between edges  $i$  and  $j$  which are distinct and nonadjacent, and  $\epsilon_k$  denotes the minimal distance from the midpoint of edge  $k$  to either of the adjacent edges  $k \pm 1$ .

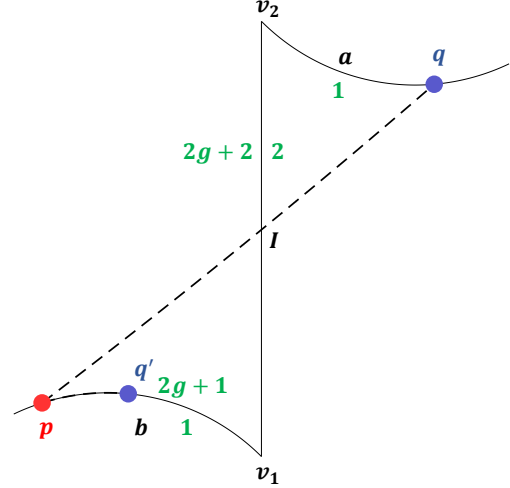


FIG. 9. Points  $p, q$  and image  $q'$  in case (1) considered in Appendix B. In this case, the geodesic  $\overline{pq}$  crosses from one polygon into another through the edge  $\overline{v_1v_2}$ . The intersection point is denoted by  $I$ . The figure shows the relevant edges from both polygons, including their common edge  $\overline{v_1v_2}$ . Segment  $\overline{pI}$  is a type I segment while  $\overline{qI}$  is a type II segment. Distances  $a = \delta(q, v_2)$  and  $b = \delta(p, v_1)$  and edge labels are also shown.

Starting once more with arbitrary points  $p \in \partial L_0$  and  $q \in \partial L_1$ , we break  $\overline{pq}$  into smaller segments so that each segment is contained in a polygon  $\gamma(P)$  and has both endpoints on its boundary. For such a segment, suppose the endpoints lie on edges with labels  $i, j$ . We categorize a segment (see Fig. 8) as

1. *type I* if  $i - j = 1$ ,
2. *type II* if  $j - i = 1$ , and
3. *type III* if  $|i - j| > 1$ .

The segments cannot be all type I, since this would imply that  $\overline{pq}$  circles around a vertex indefinitely without ever reaching  $\partial L_1$ , which cannot happen. Similarly, the segments cannot all be type II. This leaves two cases: there is either (1) a consecutive pair of type I and type II segments in either order, or (2) a type III segment. In the first case, we can show using elementary geometry that a lower bound on the combined length of the type I and type II segments, yielding a lower bound on  $\mathcal{T}$ , is

$$\mathcal{T} \geq \min \{ 2\epsilon_k \}. \quad (\text{A2})$$

In the second case,  $\mathcal{T}$  is lower bounded by the minimum length of a type III segment,

$$\mathcal{T} \geq \min \{ \delta_{ij}, |i - j| \neq 0, 1 \}. \quad (\text{A3})$$

Therefore, in either case, Eq. (A1) holds.

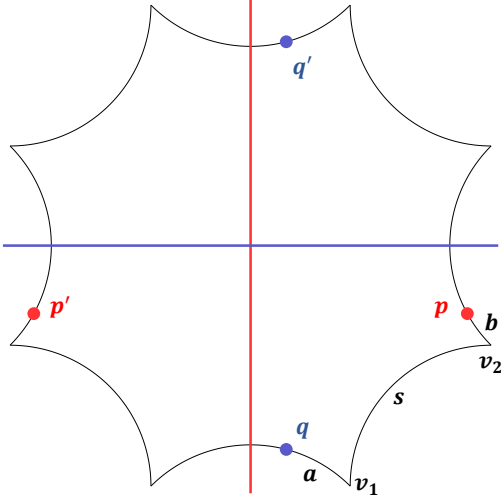


FIG. 10. Points  $p, q$  and images  $p', q'$  in case (2). In this case,  $p$  and  $q$  are on the same polygon. Perpendicular bisectors of  $pp'$  (red) and  $qq'$  (blue), vertices  $v_1$  and  $v_2$  nearest to  $p$  and  $q$ , distances  $a = \delta(q, v_1)$  and  $b = \delta(p, v_2)$ , and side length  $s$  are also shown.

### Appendix B: $k_{\min} = 1$ for the Bolza surface

In this section, we prove that  $k_{\min} = 1$  for the Bolza surface.

For an arbitrary point  $z \in P$ , it suffices to show that for any point  $w$  not in the first shell  $L_1$ , defined in Sec. III, there exists a group element  $\gamma$  such that  $\delta(z, \gamma w) < \delta(z, w)$ . Equivalently, this means that the Dirichlet polygon of  $z$  is contained inside  $L_1$ .

We prove this by contradiction. Assume that there exist points  $z \in P, w \notin L_1$  that contradict the above assertion:  $\delta(z, w) \leq \delta(z, \gamma w)$  for all  $\gamma$ . This means that  $w$  is either inside the Dirichlet polygon of  $z$  or on its boundary. Using the argument from Appendix A, the geodesic  $\overline{zw}$  must contain either

Case (1): a segment composed of a pair of type I and type II segments in either order, or

Case (2): a type III segment.

Denote the endpoints of this segment  $p, q$  such that  $z$  is closer to  $p$  than to  $q$ . Since the Dirichlet polygon of  $z$  is convex, contains  $z$  and  $w$ , and  $z, p, q, w$  are on a line,  $q$  must be in the interior of the Dirichlet polygon of  $z$ . This implies that  $z$  is in the interior of the Dirichlet polygon of  $q$ , and so by the same argument  $p$  must lie in the interior of the Dirichlet polygon of  $q$ . This means that

$$\delta(p, q) < \delta(p, \gamma q) \text{ for } \forall \gamma \neq 1. \quad (\text{B1})$$

Consider now case (1) above, where  $p$  and  $q$  are endpoints of a type I segment joined to a type II

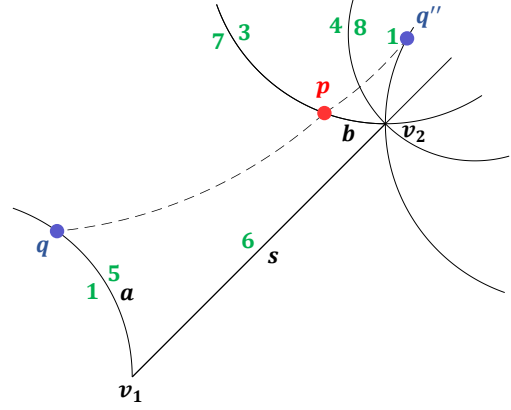


FIG. 11. Points  $p, q$  and image  $q''$  in case (2). Vertices  $v_1, v_2$ , distances  $a, b$ , side length  $s$ , and edge labels are also shown.

segment (Fig. 9). Assume without loss of generality that  $q$  is on side 1. Let  $a = \delta(q, v_2)$  and  $b = \delta(p, v_1)$ . Label-chasing, we find that there must be an image  $q'$  of  $q$  located on the same side as  $p$ . Applying the triangle inequality to triangles  $\triangle v_1 I p$  and  $\triangle v_2 I q$ , where  $I$  is the intersection between  $\overline{pq}$  and  $\overline{v_1 v_2}$ , gives

$$\begin{aligned} \delta(p, q) &= \delta(p, I) + \delta(q, I) \\ &\geq |\delta(v_1, I) - b| + |\delta(v_2, I) - a| \\ &\geq |\delta(v_1, I) - b + \delta(v_2, I) - a| \quad (\text{B2}) \\ &= |s - a - b| \\ &= \delta(p, q'), \end{aligned}$$

which is a contradiction with Eq. (B1).

In case (2), points  $p$  and  $q$  are endpoints of a type III segment, so they lie on sides of the same polygon. Consider the images  $p', q'$  of  $p, q$  located on the opposite sides of the polygon, and draw the perpendicular bisectors of  $pp'$  and  $qq'$  (Fig. 10). Observe that  $q$  must be closer to  $p$  than to  $p'$  (on the same side of the vertical perpendicular bisector as  $p$ ), and  $p$  must be closer to  $q$  than to  $q'$  (on the same side of the horizontal perpendicular bisector as  $q$ ). This is only possible when  $p$  and  $q$  are exactly 2 edges apart and lie in the same quarter-polygon, as shown in Fig. 10.

Next, assume without loss of generality that  $q$  is on side 1 (Fig. 11), and use label-chasing to determine the location of another image of  $q$ , denoted  $q''$ . Let  $a = \delta(q, v_1)$  and  $b = \delta(p, v_2)$ . From Fig. 10, we have  $0 < \{a, b\} < s/2$ . Applying hyperbolic trigonometry to quadrilateral  $pqv_1v_2$  and right

triangle  $\Delta pv_2q''$ , one can show that

$$\begin{aligned} \cosh(\delta(p, q)) &= \cosh^2\left(\frac{s}{2}\right) \cosh\left(\frac{s}{2} - b\right) \\ &\quad \times \cosh\left(\frac{s}{2} - a\right) \\ &\quad - \sinh\left(\frac{s}{2}\right) \sinh(s - a - b), \end{aligned} \quad (\text{B3})$$

$$\cosh(\delta(p, q'')) = \cosh a \cosh b. \quad (\text{B4})$$

Rearranging the first equation gives

$$\begin{aligned} \frac{\cosh(\delta(p, q))}{\cosh b} &= \sinh\left(\frac{s}{2}\right) \cosh\left(\frac{s}{2} - a\right) \\ &\quad \times \left[ \sinh\left(\frac{s}{2}\right) \tanh\left(\frac{s}{2} - a\right) \right. \\ &\quad \left. + \cosh\left(\frac{s}{2}\right) - \cosh^2\left(\frac{s}{2}\right) \right] \tanh b \\ &\quad + C, \end{aligned} \quad (\text{B5})$$

where  $C$  is a function of  $s$  and  $a$  only. The coefficient in front of  $\tanh b$  is a decreasing function of  $a$  and is negative at  $a = 0$ . It is therefore negative for all  $0 \leq a \leq s/2$ . It follows that as a function of  $b$ ,  $\cosh(\delta(p, q))/\cosh b$  is minimized at  $b = s/2$ . It also follows from Eq. (B4) that  $\cosh(\delta(p, q''))/\cosh b$  does not depend on  $b$ . To obtain a contradiction, it therefore suffices to show that

$$\frac{\cosh(\delta(p, q))}{\cosh b} \geq \frac{\cosh(\delta(p, q''))}{\cosh b} \quad (\text{B6})$$

for  $0 \leq a \leq s/2$  and  $b = s/2$ . Plugging  $b = s/2$  into

Eq. (B3) gives

$$\begin{aligned} \frac{\cosh(\delta(p, q))}{\cosh(s/2)} &= \cosh\left(\frac{s}{2}\right) \cosh\left(\frac{s}{2} - a\right) \\ &\quad - \tanh\left(\frac{s}{2}\right) \sinh\left(\frac{s}{2} - a\right). \end{aligned} \quad (\text{B7})$$

Using  $\cosh(s/2) > 1$  in the last equation, we get

$$\begin{aligned} \frac{\cosh(\delta(p, q))}{\cosh(s/2)} &\geq \cosh\left(\frac{s}{2}\right) \cosh\left(\frac{s}{2} - a\right) \\ &\quad - \sinh\left(\frac{s}{2}\right) \sinh\left(\frac{s}{2} - a\right) \\ &= \cosh a \\ &= \frac{\cosh(\delta(p, q''))}{\cosh(s/2)}, \end{aligned} \quad (\text{B8})$$

which is a contradiction completing the proof.

## ACKNOWLEDGMENTS

We thank Florent Balacheff, Maxime Fortier Bourque, Antonio Costa, Benson Farb, Svetlana Katok, Gabor Lippner, Marissa Loving, Curtis McMullen, Hugo Parlier, John Ratcliffe, and Chaitanya Tappu for useful discussions and suggestions. This work was supported by NSF grant Nos. IIS-1741355 and CCF-2311160.

- 
- [1] O. Forster, *Lectures on Riemann Surfaces* (Springer New York, 1981).
  - [2] H. Masur, *Closed trajectories for quadratic differentials with an application to billiards*, *Duke Mathematical Journal* **53**, 307 (1986).
  - [3] E. Gutkin, *Billiard dynamics: An updated survey with the emphasis on open problems*, *Chaos: An Interdisciplinary Journal of Nonlinear Science* **22**, 026116 (2012).
  - [4] J. Hadamard, *Les surfaces à courbures opposées et leurs lignes géodésiques*. *Journal de Mathématiques Pures et Appliquées* **4**, 27–74, <http://eudml.org/doc/235168> (1898).
  - [5] O. Babelon, D. Bernard, and M. Talon, *Introduction to classical integrable systems* (Cambridge University Press, 2003).
  - [6] F. Gieres, *Conformally covariant operators on Riemann surfaces (with applications to conformal and integrable models)*, *International Journal of Modern Physics A* **8**, 1 (1993).
  - [7] H.-C. Kim, S. S. Razamat, C. Vafa, and G. Zafrir, *E-string theory on Riemann surfaces*, *Fortschritte der Physik* **66**, 1700074 (2018).
  - [8] G. Bonelli, L. Bonora, F. Nesti, and A. Tomasiello, *Heterotic matrix string theory and Riemann surfaces*, *Nuclear Physics B* **564**, 86 (2000).
  - [9] B. Gustafsson and V. G. Tkachev, *The resultant on compact Riemann surfaces*, *Communications in Mathematical Physics* **286**, 313 (2009).
  - [10] E. M. Chirka, *Potentials on a compact Riemann surface*, *Proceedings of the Steklov Institute of Mathematics* **301**, 272 (2018).
  - [11] A. V. Komlov, R. V. Palvelev, S. P. Suetin, and E. M. Chirka, *Hermite–Padé approximants for meromorphic functions on a compact Riemann surface*, *Russian Mathematical Surveys* **72**, 671 (2017).
  - [12] A. Aptekarev, G. Lagomasino, and A. Martínez-Finkelshtein, *On Nikishin systems with discrete components and weak asymptotics of multiple orthogonal polynomials*, *Russian Mathematical Surveys* **72**, 3 (2014).
  - [13] A. I. Aptekarev and V. G. Lysov, *Systems of Markov*

- functions generated by graphs and the asymptotics of their Hermite-Padé approximants*, [Sbornik: Mathematics](#) **201**, 183 (2010).
- [14] X.-G. Wen and Q. Niu, *Ground-state degeneracy of the fractional quantum Hall states in the presence of a random potential and on high-genus Riemann surfaces*, [Physical Review B](#) **41**, 9377 (1990).
- [15] X.-G. Wen, *Mean-field theory of spin-liquid states with finite energy gap and topological orders*, [Physical Review B](#) **44**, 2664 (1991).
- [16] E. Aldrovandi and L. A. Takhtajan, *Generating functional in CFT and effective action for two-dimensional quantum gravity on higher genus Riemann surfaces*, [Communications in Mathematical Physics](#) **188**, 29 (1997).
- [17] J. Distler and H. Kawai, *Conformal field theory and 2D quantum gravity*, [Nuclear Physics B](#) **321**, 509 (1989).
- [18] D. Krioukov, F. Papadopoulos, M. Kitsak, A. Vahdat, and M. Boguñá, *Hyperbolic geometry of complex networks*, [Physical Review E](#) **82** (2010).
- [19] P. van der Hoorn, W. J. Cunningham, G. Lippner, C. Trugenberger, and D. Krioukov, *Ollivier-Ricci curvature convergence in random geometric graphs*, [Physical Review Research](#) **3**, 013211 (2021).
- [20] P. v. d. Hoorn, G. Lippner, C. Trugenberger, and D. Krioukov, *Ollivier Curvature of Random Geometric Graphs Converges to Ricci Curvature of Their Riemannian Manifolds*, [Discrete & Computational Geometry](#) **70**, 671 (2023).
- [21] Y. Ollivier, *Ricci curvature of metric spaces*, [Comptes Rendus Mathématique](#) **345**, 643 (2007).
- [22] M. Penrose, *Random Geometric Graphs* (Oxford University Press, Oxford, 2003).
- [23] J. Dall and M. Christensen, *Random geometric graphs*, [Physical Review E](#) **66**, 016121 (2002).
- [24] Z. Lu and X. Meng, *Erdős distinct distances in hyperbolic surfaces*, [arXiv:2006.16565](#) (2020).
- [25] M. Ebbens, I. Jordanov, M. Teillaud, and G. Vegter, *Delaunay triangulations of generalized Bolza surfaces*, [Journal of Computational Geometry](#) **13**, 125–(2022).
- [26] A. F. Beardon, *The Geometry of Discrete Groups* (Springer Science & Business Media, New York, 2012).
- [27] O. Bolza, *On binary sextics with linear transformations into themselves*, [American Journal of Mathematics](#) **10**, 47 (1887).
- [28] H. Stepanyants, A. Beardon, J. Paton, and D. Krioukov, *Diameter of Compact Riemann Surfaces*, [arXiv:2301.10844](#) (2023).